Effect of alkaline delignification process on the anatomical characteristics and some mechanical properties of tropical woods of different densities

Juan. Carlos. Maturana (jmaturana696@soyudemedellin.edu.co)
Universidad de Medellín UdeMedellín

Catalina Arroyave
Universidad de Medellín UdeMedellín

Alejandro Hurtado
Universidad de Antioquia UdeA

Félix. Echeverría
Universidad de Antioquia UdeA

Esteban Correa
Universidad de Medellín UdeMedellín

Research Article

Keywords: Partial delignification, wood chemistry, tropical hardwoods, wood modification, anatomical structure

Posted Date: October 25th, 2022

DOI: https://doi.org/10.21203/rs.3.rs-2188263/v1

Abstract

Wood delignification is a straightforward process of great interest in the development of advanced materials and products for sustainable applications. This process can reduce the stiffness of the wood cell wall by using selective chemical reagents that remove lignin/hemicellulose and thus facilitate its modification in combination with other treatments. This study aimed to compare the efficiency and uniformity of the partial delignification process using the sodium hydroxide and sodium sulfite ($NaOH/Na_2SO_3$) mixed aqueous solution in the three hardwood species *Brosimum utile* (Sande), *Carapa guianensis* (Andiroba), and *Dipteryx oleifera* (Choiba). These are important tropical tree species, providing essential material for the wood industry. The effects and distribution of the solution were studied based on the variations exhibited by the center and ends of the delignified woods, using chemical composition analysis techniques, FT-IR spectra, optical microscopy, and scanning electron microscopy (SEM). The process allows the partial chemical removal of lignin/hemicellulose in different non-uniform proportions between the center and the ends of the woods under study. The lignin/hemicellulose removal ratios varied widely between the different wood species. The density of delignified wood did not vary significantly after treatment. The modulus of rupture (MOR) and modulus of elasticity (MOE) of delignified wood decreased. The results suggested that denser tropical wood requires the adjustment of the process variables while the proposed method can treat less dense tropical woods. Partially delignified tropical hardwood can be used to develop advanced materials and products for diverse applications.

1. Introduction

Anatomical structure is a critical factor influencing the efficiency of chemical pretreatment of wood. It is generally believed that material with bigger surface area can be pretreated more easily. The complex lignocellulosic plant cell wall, with highly crystalline lignin, heterogeneous hemicelluloses, cellulose, and their interactions extend influence on its recalcitrance (Zhu et al. 2022). Delignification is an effective technique for removing lignin content from the wood. This technique is in industrial use (Kumar et al. 2021), and recently has been used in combination with other wood modification techniques to promote new advanced materials and wood-based products (Grönquist et al. 2019; Chen et al. 2020a) such as highly elastic hydrated cellulosic materials (Chen et al. 2020b), photostable transparent wood composite (Bisht et al. 2021), highly compressible wood carbon sponge (Chen et al. 2018), and densified wood (Shi et al. 2020). More specifically, in the densification process, delignification is used as a pretreatment technique for softening the cell wall of the wood. This technique is an alternative to the temperature elevation softening used in thermo-mechanical (TM) densification (Kutnar et al. 2015; Jakob et al. 2022), the use of steam in thermo-hydro-mechanical (THM) treatment (Sandberg et al. 2012; Jakob et al. 2022), the use of pressurized steam in the viscoelastic-thermal-compression (VTC) process (Albert and Liew 2020; Wang et al. 2021a; Jakob et al. 2022), or to polymer impregnation of polymer-infiltrated compressed wood (Shams et al. 2005; Jakob et al. 2022). This delignification process favors the compression of the anatomical structure of wood (Frey et al. 2018) and contributes to improving the mechanical behavior of the wood through the partial removal of lignin (Shams et al. 2005; Frey et al. 2018; Shi et al. 2020; Jakob et al. 2020). However, to the best of our knowledge, the literature referring to the delignification process

does not provide information on the uniformity of partial lignin removal from the anatomical wood structure. In this context, exploring the effects and behavior of woods during partial delignification is highly desirable, especially in order to better understand the pretreatment, given the growing interest in developing advanced wood-based materials and products for sustainable applications.

This pretreatment removes lignin in wood (Singh et al. 2014; Okur and Eslek Koyuncu 2020; Kumar et al. 2021) by accessing the polymeric matrix of lignin, hemicellulose, and cellulose in the ultrastructure (Frey et al. 2019). For this purpose various chemical solvents, such as alkaline reagents, acids, and ammonia, reduce the rigidity of the lignocellulosic structure (Zhao et al. 2022; Jamaldheen et al. 2022). Alkaline reagents derived from the hydroxyl of sodium, potassium, calcium, and ammonium salts are used (Kumar and Sharma 2017). The most used alkaline reagent for the pretreatment is sodium hydroxide. This is an effective chemical agent as it can expose cellulose to a greater degree than other chemical reagents (Rabemanolontsoa and Saka 2016), as it is a selective reagent to dissolve lignin and hemicellulose while retaining cellulose and increasing wood porosity (Kim et al. 2016). As a result of these characteristics, sodium hydroxide has been widely used to develop different versatile materials and products, such as super flexible wood (Song et al. 2017), transparent wood composite (Bisht et al. 2021), elastic wood (Chen et al. 2020b), and wood aerogel (Song et al. 2018a). Recently, Song et al. (2018) employed a mixed aqueous solution of sodium hydroxide and sodium sulfite as a pretreatment to soften the cellular structure before mechanical compression. They found that, in addition to reducing the mechanical strength of the hierarchical wood structure, the pretreatment process allows the complete collapse of this structure during densification and increases the strength properties of the wood. Currently, both hardwoods and softwoods are used in this process, and their selection varies depending on the final application (Kumar et al. 2021). For example, balsa wood is widely used in the development of phase change materials (Meng et al. 2020), in biocomposites (Chen et al. 2021), and in the manufacture of transparent wood (Wang et al. 2021b). Poplar (Song et al. 2018b; Wang et al. 2020), basswood, oak, western red cedar, eastern white pine (Song et al. 2018b), birch (Mania et al. 2020), and spruce (Jakob et al. 2020), among others, are used in the manufacture of densified wood.

The previously cited works provide an exciting overview of the use of some softwoods and hardwoods in wood modification with preliminary delignification. One motivating factor for these works is the environmental advantage of using abundant and available woods with specific strength properties. For the same reason, the present study evaluates the delignification process using three tropical hardwoods with specific characteristics. The selected species have distinctive attributes, availability in the region, and are tropical hardwoods that are part of Colombia's forest potential, widely used in furniture, construction, decorative elements, and tool handles in the domestic market. *Brosimum utile* (Sande), *Carapa guianensis* (Andiroba), and *Dipteryx oleifera* (Choiba) are three important hardwood species belonging to the botanical families *Moraceae*, *Meliaceae*, and *Fabaceae*, respectively. They are native to the forests of the biogeographic region of Chocó in western Colombia, where they grow under conditions of extreme precipitation and high humidity, among other aspects particular to the region (Pérez-Escobar et al. 2019). While softwoods are composed primarily of one cell type (Shi et al. 2020), hardwood species have a more complex anatomical and chemical structure (E. Wheeler 2001; Mamoňová and Reinprecht 2020), making

the wood modification process challenging. Therefore, to understand delignification treatment in tropical hardwoods with potential for the development of the eco-friendly materials and products of interest, it is necessary to understand how the distribution of the delignification solution influences the softening of the anatomical structure of bulk wood. Consequently, this study aims to compare the uniformity and efficiency of the partial delignification process of NaOH/Na_2SO_3 mixed aqueous solution in tropical hardwoods through the sectioned study of bulk wood, to elucidate the homogeneity and treatment effects on the anatomical structure of delignified wood (DW). This study was expected to provide a knowledge base that will help understand how different variables of the partial delignification process affect the anatomical structure of delignified wood, for the development of densified wood as an advanced wood-based material.

2. Materials And Methods

2.1. Materials and Chemicals

Sande (*Brosimum utile*), Andiroba (*Carapa guianensis*), and Choiba (*Dipteryx oleifera*) tropical wood species were used for the delignification process. The dimensions of the specimens were set at 30 × 30 × 100 mm^3 (radial × tangential × longitudinal) and they were kiln-dried at a constant weight at 103°C for 24 h before use. Sodium hydroxide (≥ 99,0%) and sodium sulfite (≥ 97%) were purchased from Merck (Canada). Deionized (DI) water was used as the solvent to process the wood. All chemicals were used as received.

2.2. Analysis of delignified wood

Firstly, the delignification process with alkaline solution reported by Song et al. (2018) was carried out. The specimens were immersed in a boiling mixed aqueous solution of 2.5 M, NaOH and 0.4 M Na_2SO_3 at 90°C for 7 h, followed by immersion in boiling DI water several times to remove the excess of chemical reagents. Next, the DW was oven-dried at 50°C for one week at constant weight. Then, the DWs were evaluated from samples divided into two sections: *ends* and *center*, respectively, as shown in Fig. 1. The limits were established as the perimeter area of the center of the cross-sectional bulk wood. From the central section in a longitudinal direction, 15 mm ends were extracted from the edge to the center of the unit. The center was calculated as the central intersection of the base division and the height of the samples at 4/4 in their cross-section.

2.3. Measurements and Characterizations

The FT-IR spectrum was collected using an FTIR spectrometer (Spectrum Two, PerkinElmer, MA, USA) equipped with an ATR module, recording over a range of 4000 – 450 cm^{-1} at a resolution of 4.0 cm^{-1} and taking the average of 24 scans for each specimen. The untreated wood and DW were prepared as thin sections, with thickness lower than 1 mm. One measurement was performed per sample. The spectra were recorded as transmittance versus wavenumber to find the effect of the delignification process on the

pieces and identify the presence of functional groups that could be present in the sample. The partial removal of the chemical components of the specimens was quantitatively examined according to Van Soest et al. (1991). Ash composition was determined by the volatilization losses method according to the NTC 5167 standard. The microstructure of the untreated wood and DW was observed under the optical microscope (Olympus BX50F4), and the anatomy of the detected fibers, vessels, and rays was described using the International Association of Wood Anatomists (IAWA) List of Features for Hardwood Identification (IAWA Committee 1989). The surfaces of the samples were prepared in cross-section, and the generated images were analyzed using Motic Images Plus 3.0 software. Twenty-five lumen and fiber wall thickness measurements were counted from different cross-sectional areas. Then, scanning electron microscope (SEM, JEOL JSM-6490LV) at 20 kV was used to reveal the morphologies of the wood samples. The observed characteristics were measured by SEM analysis and using the image analysis ImageJ software (Schneider et al. 2012). The basic specific weight (density) was measured in 5 wood samples for each species before and after the delignification process. The apparent volumetric mass density of the samples was calculated using the following equation: $\rho_{Wood} = m/V$, where *m* is the weight and *V* is the volume of the specimens before and after the delignification process, respectively. The porosity of the specimens was calculated based on the dried sample mass and solid wood before and after delignification. Porosity was calculated with the following equation:

$$\text{Porosity}\,(\%) = \left(1 - \frac{\rho_{\text{wood}}}{\rho_{\text{s}}}\right) \times 100$$

Where ρ_{wood} and ρ_s are the volumetric mass densities of the wood and solid wood, respectively. According to the previous study, the density value of solid wood (cell wall) of 1500 kg m^{-3} was used (Gibson 2012). The absorption capacity of the samples was determined by measuring the increase in weight relative to their dry state. The natural wood samples were cut into cubes with dimensions of 3 × 3 × 3 mm^3 (radial × tangential × longitudinal) and dipped into 1000 ml of running water for 30 min. At least five replicates were measured to calculate the average value. The absorption capacity (g/g) was calculated as follows:

$$\text{Absorption}\,(\text{g/g}) = \frac{\text{m}_1 - \text{m}_0}{\text{m}_0}$$

Where m_0 and m_1 are the sample's dry mass and final mass during water absorption, respectively. The mechanical properties of the untreated and delignified specimens were evaluated using a Tinius Olsen testing machine with a capacity of 15000 kg. The modulus of rupture (MOR) and modulus of elasticity (MOE) in compression parallel to the grain were measured according to the NTC 784 standard (Icontec 2019a), using three specimens from each species, prepared with the dimensions of the cross-section of 30 x 30 x 100 mm^3 in longitudinal direction. Janka's hardness method was used to measure the hardness before and after the delignification according to NTC 918 (Icontec 2019b). Three samples were analyzed with 30 x 30 x 100 mm^3 cross-section and longitudinal dimensions.

2.4. Statistical analysis

Data from this study were analyzed using Statgraphics Centurion 19. A correlation analysis was performed between the lumen diameters of the wood fibers and the degree of delignification of the treated woods. An analysis of variance (ANOVA) was applied with $P \leq 0.05$ being significant.

3. Results

Figure 2 shows the FT-IR spectra and the relative content of cellulose, hemicelluloses, and lignin of the selected hardwoods of medium and high density that were used to study the delignification process. The chemical composition and basic density values of the natural wood of the three species are shown in Table 1. According to these results, it can be observed that the lignin content of these woods is greater than 30%. The delignification process was performed similarly in all specimens using the mixed aqueous solution of $NaOH/Na_2SO_3$. In this process, both the temperature at 90°C and the time of seven hours had significant effects on the removal of lignin and hemicellulose in two species (Sande and Andiroba*)*, which are the lower-density woods, while in the higher-density wood (Choiba) this behavior was not observed. FT-IR analysis was carried out to confirm the DW removal of lignin and hemicellulose. The identified spectra are shown in Fig. 2a. Initially, a broadened absorption band located at 3337 cm^{-1} for the (-OH) phenolic hydroxyl groups can be observed in each wood. The band located at 2891 cm^{-1} is due to the presence of the C-H stretching vibration in cellulose, hemicellulose, and lignin. The band located at 1736 cm^{-1} corresponds to (C = O) stretching vibration in carbonyl groups of hemicellulose/lignin, and the bands located at 1593 and 1505 cm^{-1} are due to the (C = C) aromatic skeleton vibrations rings in lignin. The band located at 1419 cm^{-1} is due to the presence of the C – H stretching in lignin and carbohydrates and 897 cm^{-1} for C – H deformation in cellulose. The absorbance bands located at 1261, 1235 and 1028 cm^{-1} correspond to C – O stretching vibration. The absorbance band located at 1155 cm^{-1} corresponds to the symmetric (C–O–C) stretching vibration in cellulose/hemicellulose. Figure 2b compared the FT-IR spectra of natural wood and DW. The bands located at 1736 and 1235 cm^{-1} for carbonyl stretching and C – O stretching are significantly reduced for Sande and Andiroba. For Choiba, no peaks were observed located at 1736 and 1235 cm^{-1}, and the region showed no significant difference between these bands observed after chemical treatment.

For all three species after chemical treatment, no significant reduction in the intensity of the bands located at 1593 and 1505 cm^{-1} for the aromatic skeleton in lignin was observed, suggesting that this should be verified by a quantitative method. The chemical composition analysis quantified lignin and hemicelluloses at the ends and center samples. Figure 2c-e shows the relative chemical composition content after chemical treatment of the center and the ends of the three types of wood, respectively. The results confirmed a partial lignin removal of approximately 47.4% for Sande and 73.7% for Andiroba, while there was no significant lignin removal for Choiba. Lignin was also found to concentrate towards the ends of the samples compared to the center after treatment. The process also shows slight hemicellulose removal for Choiba (5%) and Andiroba (9%). However, hemicellulose removal was significantly high in the Sande (> 90%). Meanwhile, hemicellulose content is higher at the center than at the ends for Sande and Choiba. In Andiroba, the opposite behavior was observed.

Table 1
Chemical composition, density, and absorption capacity of natural woods.

Samples	Family	Cellulose (%)	Hemicellulose (%)	Lignin (%)	Basic density (g/cm^3)	Absorption capacity (g/g)	Fiber luminaire's diameter (μm)
Sande	Moraceae	47.6 ± 0.7	12.1 ± 0.2	31.2 ± 0.9	0.44 ± 0.01	0.14 ± 0.009	41.24 ± 9.02
Andiroba	Meliaceae	34.0 ± 1.0	12.13 ± 0.06	35.7 ± 0.7	0.50 ± 0.01	0.08 ± 0.009	40.96 ± 9.30
Choiba	Fabaceae	32.0 ± 2.0	10.6 ± 0.8	34.8 ± 0.2	0.94 ± 0.04	0.03 ± 0.003	5.12 ± 3.36

The results of the analysis of ash content in natural and delignified wood are shown in Table 2. In our results, the ash content was significantly higher after chemical treatment for all samples, both at the center and at the ends. It is observed that the percentage of ash in the samples with the $NaOH/Na_2SO_3$ treatment increases in a more considerable proportion at the extremes than in the center. As a comparison, Sande showed the most significant difference in ash increase at the ends after chemical treatment. At the same time, the samples of Choiba showed the smallest increase.

Table 2
Results of partial delignification on the physical properties of natural wood and some chemical elements.

Sample	Parameter	Natural wood	Delignified wood	Rate D/N
Sande	The density of woods (g/cm^3)	0.55 ± 0.002	0.59 ± 0.015	1.1
	Porosity (%)	63.5 ± 0.16	60.7 ± 0.98	1.0
	Total ash content (%)	0.55	7.26	13.2
	Center ash content (%)		1.7	
	Ash content at the ends		8.09	
	Total Calcium (CaO) (%)	0.184	0.1452	0.8
	Magnesium (MgO) (%)	0.0552	0.048	0.9
	Sodium (Na) (%)	0.009	2.14	237.8
	Potassium (K_2O) (%)	0.103	0.0351	0.3
	Sulfur (S) (%)	0.090	0.303	3.4
Andiroba	The density of woods (g/cm^3)	0.55 ± 0.007	0.59 ± 0.016	1.1
	Porosity (%)	63.6 ± 0.47	60.4 ± 1.04	0.9
	Total ash content (%)	1.02	8.34	8.2
	Center ash content (%)		0.98	
	Ash content at the ends		4.98	
	Total Calcium (CaO) (%)	0.3835	0.338	0.9
	Magnesium (MgO) (%)	0.0416	0.0429	1.0
	Sodium (Na) (%)	0.0086	2.29	266.3
	Potassium (K_2O) (%)	0.0471	0.0353	0.7
	Sulfur (S) (%)	0.096	0.184	1.9
Choiba	The density of woods (g/cm^3)	1.06 ± 0.006	1.05 ± 0.011	1.0
	Porosity (%)	29.6 ± 0.42	30.3 ± 0.76	1.0
	Total ash content (%)	1.23	9.69	7.9
	Center ash content (%)		1.33	
	Ash content at the ends		3.12	
	Total Calcium (CaO) (%)	0.5306	0.399	0.8

Sample	Parameter	Natural wood	Delignified wood	Rate D/N
	Magnesium (MgO) (%)	0.0497	0.051	1.0
	Sodium (Na) (%)	0.00821	1.56	190.0
	Potassium (K_2O) (%)	0.0452	0.0202	0.4
	Sulfur (S) (%)	0.079	0.066	0.8

The procedure also caused significant changes in the surface of the wood. It was found that the DW samples were darker in color after the delignification treatment. In addition, a darker region at the ends compared to the center was observed in the delignified samples. Figure 3 shows the morphology and structure of the three different wood samples while in Fig. 4 the effects of partial delignification on wood structure (Sande and Andiroba) are shown. The vessels in Sande wood were diffuse-porous, visible to the naked eye, solitary, and in short radial multiples of 2–3, with frequency of ≤ 5–20 vessels per square millimeter. In the vessels, simple perforation plates were observed. In cross-sections, axial parenchyma winged-aliform was also observed. Rays in the Sande wood are heterocellular, and visible to the naked eye on the radial and tangential sections. In tangential sections, 4 to 10 seriate rays predominated. The fibers in Sande wood were made up of non-septate fibers, thin- to thick-walled with a large lumen (Fig. 3d). The fiber luminaire's mean diameter is shown in Table 1. The growth ring in Andiroba wood was of distinct boundaries, defined by terminal parenchyma bands and pore concentration. The vessels were diffuse-porous, visible to the naked eye, solitary, and in radial multiples of 2–3, or occasionally 2–4, with frequency of ≤ 5–20 vessels per square millimeter, and some rare clusters vessel common (vessels with whitish contents and dark brown gums). In the vessels, simple perforation plates were observed. In cross-sections, axial parenchyma and scanty paratracheal and axial parenchyma in marginal or seemingly marginal bands were also observed. Rays in the Andiroba wood were visible to the naked eye on the tangential sections; 4 to 10 seriate rays prevailed. Also, axial canals in long tangential lines and intercellular canals of traumatic origin were observed (arrows within the yellow rectangle of dashed lines in Fig. 4e). The fibers in Andiroba wood were made up of septate fibers, thin- to thick-walled with a large lumen (Fig. 3e). The fiber luminaire's mean diameter is shown in Table 1. The vessels in Choiba wood were diffuse-porous, visible to the naked eye, in a diagonal and radial pattern, with radial multiple groupings of 4 or more and some rare solitary vessels, and frequency ≤ 5–20 vessels per square millimeter. In the vessels, simple perforation plates were observed. In cross-sections, axial parenchyma winged-aliform was also observed. Rays in the Choiba wood are not visible with the naked eye on the tangential surface but contrasted in the radial sections, with ray width of 1 to 3 cells. The fibers in Choiba wood were made up of non-septate fibers, very thick-walled, with a small lumen (Fig. 3f). According to these results, both the structure of the vessels and the fibers retain their shape. In general, in the analyzed samples, a tangential diameter of vessel lumina was found in the range of 100–200 μm, with 5–20 vessels per square millimeter. The fiber luminaire's mean diameter is shown in Table 1.

High-resolution SEM images (Fig. 3j-l) showed that the cellular structure of the DW preserved the morphology and microscopic features of the honeycomb structure of natural wood. After partial removal

of lignin and hemicellulose, the vessels in the cross-section of the DW in the three species retained their round or oval shape. The fibers in Choiba wood were very thick-walled, ≥ 5 μm. Meanwhile, the fibers in Sande and Andiroba were thin-to-thick-walled, ≤ 3 μm. Fiber cell detachments from delignification were observed (yellow arrows in Fig. 4a-d). The effect of delamination in intercellular channels after the delignification process was also observed at the ends of Andiroba (yellow arrows in Fig. 4f).

The results of the evolution of the physical properties of the DW are summarized in Table 2. According to these results, it can be determined that the density does not have a significant increase after $NaOH/Na_2SO_3$ treatment. The highest density increase was 0.05 g/cm^3 in Sande and Andiroba samples. Regarding Choiba specimen, the density slightly decreased after delignification process. The chemical treatment did also not have significant effects on the porosity of the woods. The highest variation in porosity was 3.2%, in Andiroba. The highest porosity was observed in the lowest density woods. It was found that the porosity decreases in the lowest density woods with the partial removal of lignin and hemicellulose. The adsorption capacity of natural wood samples is shown in Table 1. According to these results, lower density samples have better behavior. The 30-minute water absorption of natural wood showed density 4.8 times lower for the densest wood than for the least dense wood.

The mechanical properties of the untreated and delignified specimens are presented in Fig. 5. As expected, the strength of the three wood specimens decreases with the partial delignification process. Figures 5a and b compare both MOR and MOE of natural wood and DW for the three specimens. For Sande, after the delignification process there are significant reductions in both MOR and MOE of about 46 and 80%, respectively, while for Andiroba, these reductions are observed to be 24 and 31%, respectively. The reductions for Choiba were 2 and 49%, respectively. The average values of each specimen's hardness, in both natural wood and DW, are presented in Figs. 5c and d. The surface hardness of DW compared to that of the natural wood decreases by 12, 38, and 42%, for Sande, Andiroba, and Choiba, respectively. Likewise, the hardness at the ends of the DW was reduced by 34, 34, and 48% for Sande, Andiroba, and Choiba, respectively.

4. Discussion

Delignification is an uncomplicated process used in wood modification that relies on several variables to achieve its component removal effect, whereby lignin and hemicellulose are removed from the lignocellulosic matrix, while cellulose is retained (Grönquist et al. 2019). In this study, the delignification process was performed according to the method reported by Song et al. (2018) as a densification pretreatment. The alkaline chemical removal treatment had different effects on the removal of chemical components in natural wood (Kim et al. 2020) of the three species. The amount of lignin removed was much higher for Andiroba species than for Sande species, whereas for hemicellulose, the amount removed was higher in the Sande species than in the Andiroba species. (Fig. 2d-f). Conversely, for Choiba species, the alkaline treatment had no appreciable effect on the removal of either lignin or hemicellulose. Based on this, we suggested that the anatomical and chemical composition of the studied woods may influence both the heterogeneous distribution and the effects of the alkaline chemical solution within the

anatomical structure of wood. Therefore, the efficiency of the partial delignification method by means of $NaOH/Na_2SO_3$ solution was then later analyzed through the variations exhibited by the center and the ends of the DW (schematic overview in Fig. 1).

The results indicated that the tangential luminal diameter of vessels of Sande, Andiroba, and Choiba was the same, while fibers showed a mean luminal diameter that was similar in Sande and Andiroba but significantly different in Choiba (Table 1). Smaller fiber lumen has been associated with higher density wood as the Choiba species (Thomas et al. 2007; Mamoňová and Reinprecht 2020). Also, the thicker the cell walls, the higher the density (Zanne et al. 2010). In the present study, Choiba is the wood with the highest density and presents the highest cell wall thickness in fiber cells (Table 1). This variation between the fiber lumens of the wood could be related to the removal of lignin and hemicellulose in Choiba wood being the lowest of the three woods studied. This observation suggests that the efficiency of the delignification process in Choiba wood was limited by the fiber morphology of narrow lumens and very thick walls (Fig. 3d-i), in contrast to the Sande and Andiroba anatomical structure of wide lumen fibers and thinner walls. In Choiba, it is probable that narrow pores in the channel restrict the passage of the alkaline solution penetration into the wood (Brännvall 2017). When comparing the anatomical features of the three species, we observed that the structure plays a pivotal role in the efficiency of the delignification process.

Despite the morphological similarities between Sande and Andiroba, the percentage of delignification was not similar in both species. The difference in the efficiency of the delignification process between Sande and Andiroba is due to the wood structure of Andiroba. This is because Andiroba, among its anatomical features, has common vessel clusters and traumatic resin canals (intercellular canals) (Wheeler 2011) (Fig. 4e, f). Resin channels are common in the *Meliaceae* species family to which Andiroba belongs (Dünisch and Baas 2006). Resin canals allow the alkaline solution to be more homogeneous in the wood, which provides additional openings for a longitudinal flow of the solution (Brännvall 2017; Wagih et al. 2021). The resin canals could have facilitated the flow of the alkaline solution into the Andiroba wood. Thus, it is possible that the higher lignin removal effect in Andiroba may be attributed to a higher content of morphological features that are beneficial for alkaline solution flow.

In the delignification process, a key factor besides the anatomical structures of wood is the cellular chemical composition, since lignin is a complex amorphous polymer (Boerjan et al. 2003; Lu et al. 2017). Chemical removal of lignin was achieved by complex chemical reactions generated by the encounter of $NaOH/Na_2SO_3$ aqueous solution with the monomeric lignin units (Li et al. 2021). NaOH is alkaline reagent that fractionates lignin and hemicellulose. Sodium hydroxide breaks the ether and ester linkages of lignin-carbohydrate complexes (LCC) and the ester and carbon-carbon (C-C) linkages of lignin molecules (Kim et al. 2016). Meanwhile, Na_2SO_3 contributes to lignin dissolution and decreases the process duration. Also, hemicellulose is removed by the $NaOH/Na_2SO_3$ solution (Kim et al. 2020). Indicative of these chemical changes is the loss of the natural luster of delignified wood. This is an effect that has been reported in other studies (Song et al. 2018a; Guan et al. 2018; Yang et al. 2020), and is attributed to the breaking of chemical bonds and removal of extractives (Shi et al. 2018), as well as to the removal of chromophores

from the lignin (Meng et al. 2020).In this study, it was observed in FTIR analysis that the bands located at 1736 and 1235 cm^{-1} in Sande and Andiroba wood (Fig. 2b) showed a reduction in peak areas after the delignification process. These peak areas are similar to natural and delignified Choiba wood. The spectra bands at 1736 cm^{-1} are attributed to acetyl-xylan when tentatively assigned to xylan (hemicellulose) and ρ-coumaric acids of lignin (Md Salim et al. 2021). The band centered at 1235 cm^{-1} was assigned to the C-O stretching of the guaiacyl unit in lignin (Zhuang et al. 2020). These reductions in band intensities were due to the fact that the heating process with the alkali solution may cause cleavage of the β-O-4 bond, which is the primary bond in lignin, and removal of the acetyl groups of galactoglucomannan (Horikawa et al. 2019).

FTIR spectroscopy showed that the delignification process had been successful since lignin and hemicellulose were partially removed. Consistently with this, there are studies on the delignification process aside from the removal of the lignin, where part of the hemicellulose was removed (Kim et al. 2020; Li et al. 2021). Meanwhile, the intensity of peak areas at 1593 and 1505 cm^{-1} increased in the three wood species, indicating that a significant proportion of lignin remained in the wood structure. This lack of reduction in the intensity of the peaks at 1593 and 1505 cm^{-1} for the aromatic skeleton in lignin is because only a partial amount of lignin was removed. This was corroborated by the quantified method (Figs. 2c, d, and e).

Although several FTIR bands of different wood components overlapped, the IR spectra of the three kinds of wood still provide information about changes in chemical composition after delignification. In the three species of woods, the intensities of the band at 1028 cm^{-1} (Fig. 2b) were similar after alkaline treatment, which indicates that the cellulose was not removed (Da Costa et al. 2021). Nonetheless, the general structure indicated by the stretch vibrations of specific molecular bonds between natural woods were similar in absorption bands wavenumbers of the FTIR spectrum (Fig. 2a).

Another parameter that can influence the rate of delignification is the presence of inorganic, non-soluble salts (non-process elements), for example, high calcium content in wood makes it challenging to delignify (Senthilkumar 2019). Thus, mineral content could have had a negative effect on the removal of lignin in Choiba, where the calcium content was higher than in Sande and Andiroba (Table 2).

Calcium ions (Ca^{+2}) can form an intermolecular bond with homogalacturonan (HG) molecules to form rigid structures known as the "egg crate model" (Siedlecka et al. 2008). The native cell walls generate demethylation in the C-6 carboxyl of the HG stretches, thus creating rigid structures of pectin-calcium-pectin that stabilize the pectin network. Pectin methyl esterase enzymes are involved in this process, through mechanisms related to the determination of the width and length of the fiber in the wood. Thus, less methylated lignin formation of eggshell structures influences the plasticity of the wall (Siedlecka et al. 2008), a quality that can influence the delignification process. In Choiba, the spectra bands located at1028 and 897 cm^{-1} are attributed to demethylated lignin (Ferhan, M., Yan, N., & Sain 2013), in contrast to the lowest diameter of the luminaire fiber (Table 2), which is related to the low efficiency of the delignification process. These parameters exhibited higher values in Andiroba and Sande. The sulfur

content of the delignified wood is about 3.4 times higher than that of natural Sande wood, while in delignified Andiroba wood it was 1.9 times higher than natural wood (Table 2). This was probably because Na_2SO_3 solution contributed to lignin demethylation through nucleophilic attacks and $-OCH_3$ groups were removed by a nucleophilic substitution reaction (Li et al. 2016). In this study, the impregnation of the alkaline solution was analyzed in the delignification process of each wood (Fig. 2c, d, e). Wood samples were separated between the center and end (Fig. 1). The results indicated that the delignification was heterogeneous between the center and the ends in Sande (Fig. 2c).

As the internal structure of the wood is conditioned by pores and lumens of different sizes, the higher delignification in the center of the samples can be explained by a longer reaction time of the alkaline solution in the center of the samples. However, the possibility of lignin measurements obtained in the delignified samples being influenced by the unusual deposition of fragmented lignin at the ends of Sande and Andiroba is not excluded, since the dissolution residue could contain lignin (Sun et al. 2009).

With regard to the anatomical structure after treatment, the delignified samples retained their porous structure, and the fibers and vessels in the dry state maintained their circular or oval shape (Fig. 3j-l). However, partial lignin removal in the middle lamella caused a separation between adjacent cell walls (Fig. 4a-d). These effects are consistent with previous research findings that attribute cell wall separation to lignin removal from the middle lamella (Wu et al. 2019). At the same time, microcracks were observed in some fiber cells of Sande (Fig. 4a), due to the partial removal of lignin from the cell wall. Another effect after treatment is the loss of the natural luster of DW, which functions as an indicator of chemical changes. This effect is assigned to the removal of chromophores from the lignin (Meng et al. 2020), breaking of chemical bonds, and removal of extractives (Shi et al. 2018). Other studies also have reported these effects (Song et al. 2018a; Guan et al. 2018; Yang et al. 2020).

Finally, this study evaluated the physical and mechanical properties of delignified wood. Regarding the physical properties of delignified wood, no significant variations were observed in the density or porosity of the samples, given the loss of mass was not significant. It is likely that porosity was affected beyond the scope of the measurement method used here, as increased porosity due to lignin removal has been widely reported (M. Frey et al., 2019; Guan et al., 2018; A. Kumar et al., 2021). On the other hand, the chemical degradation of the chemical constituents of wood reduced some mechanical properties (Fig. 5). However, the chemical components of wood contribute to the mechanical properties (Shi et al. 2020). Specifically, lignin acts as a micro/nanoscale binder in the wood cell wall (Jungstedt et al. 2020), which preserves structural integrity by providing stiffness and strength (Kumar et al. 2021), while hemicelluloses act as a crosslinking agent between cellulose and lignin in the cell wall, which influences its mechanical properties (Kumar et al. 2021)). Therefore, the mechanical properties are reduced after the removal of lignin and hemicellulose (Kumar et al. 2021). Furthermore, these mechanical properties are affected by the removal of ash, since this involves the removal of silicon, which is one of the components of ash that favors plants' natural and mechanical resistance (Xu 2010).Therefore, as expected, the removal of lignin, hemicellulose, and ashes through the delignification process affected the mechanical resistance of the treated woods (specially Sande and Andiroba). Thus, it was suggested that the removal of lignin allows

the delignified wood to be efficiently compressed (Shi et al. 2020). These conditions are what was expected for the development of subsequent treatments such as densification.

5. Conclusions

In summary, of the three tropical hardwood samples evaluated, the two species with the lowest density, corresponding to Andiroba and Sande, were partially delignified with the alkaline chemical treatment of $NaOH/Na_2SO_3$ mixed aqueous solution. The anatomical results indicated that the morphology of the coarse fibers impedes the flow of the alkaline solution into the interior of high-density woods such as Choiba; therefore, Choiba wood had no delignification effects. On the other hand, anatomical defects such as intercellular resin channels present in Andiroba wood contribute to a greater delignification effect. FTIR analyses confirmed the variation of lignin-carbohydrate binding functional groups through chemical degradation of hemicellulose and lignin in the cell walls and middle lamella of delignified woods. Sectioned analysis of the center and ends of delignified samples confirmed that alkaline chemical treatment is a process with non-uniform effects on lignin and hemicellulose removal in the anatomical wood structure. Lignin removal was higher in the center of delignified samples than at the ends. In this study, the removal of lignin and hemicellulose, as ash and wood extracts, reduced MOE, MOR, and the hardness of delignified wood, but not wood density. The above results suggest that medium-density tropical hardwood can be readily delignified using the studied method. High-density tropical hardwood should be subjected to different conditions to achieve a delignification effect that will allow its use with other wood modification strategies to develop advanced wood-based materials.

Declarations

CRediT authorship contribution statement

All the authors listed contributed to the completion of this research. Juan C. Maturana: Data collection and analysis, Methodology, Investigation, Validation, Writing – original draft. Catalina Arroyave: Conceptualization, Methodology, Supervision, Investigation, Formal analysis, Validation, Visualization, Writing – review & editing. Alejandro Hurtado: Conceptualization, Methodology, Writing - review & editing. Felix Echeverría: Formal analysis, funding acquisition, Writing review & editing. Esteban Correa: Formal analysis, Funding acquisition, Validation, Visualization, Writing – review & editing. Project administration.

Declaration of Competing Interest

The authors declare that they have no known competing financial interests or personal relationships that could have influenced the work reported in this paper.

Acknowledgments

Universidad de Medellín and Universidad de Antioquia supported this study [Project No. 1061]. Juan C. Maturana acknowledges Gobernación del Chocó, Universidad Tecnológica del Chocó and Sistema

General de Regalias [Project, BPIN: 2014000100035] for the doctoral fellowship [Convocation 2-2017, contract 0026-2017].

References

1. Albert CM, Liew KC (2020) Effect of viscoelastic thermal compression (VTC) treatment on density and moisture content of laminas from Paraserianthes falcataria. Adv Mater Process Technol. https://doi.org/10.1080/2374068X.2020.1799574
2. Bisht P, Pandey KK, Barshilia HC (2021) Photostable transparent wood composite functionalized with an UV-absorber. Polym Degrad Stab 189:109600. https://doi.org/10.1016/j.polymdegradstab.2021.109600
3. Boerjan W, Ralph J, Baucher M (2003) Lignin biosynthesis. Annu Rev Plant Biol 54:519–546. https://doi.org/10.1146/annurev.arplant.54.031902.134938
4. Brännvall E (2017) The limits of delignification in kraft cooking. BioResources 12:2081–2107. https://doi.org/10.15376/biores.12.1.2081-2107
5. Chen C, Kuang Y, Zhu S, et al (2020a) Structure–property–function relationships of natural and engineered wood. Nat Rev Mater. https://doi.org/10.1038/s41578-020-0195-z
6. Chen C, Song J, Cheng J, et al (2020b) Highly elastic hydrated cellulosic materials with durable compressibility and tunable conductivity. ACS Nano 14:16723–16734. https://doi.org/10.1021/acsnano.0c04298
7. Chen C, Song J, Zhu S, et al (2018) Scalable and sustainable approach toward highly compressible, anisotropic, lamellar carbon sponge. Chem 4:544–554. https://doi.org/10.1016/j.chempr.2017.12.028
8. Chen Q, Jiang Z, Pei X, et al (2021) Bio-inspired, epoxy-based lamellar composites with superior fracture toughness by delignified wood scaffold. Compos Sci Technol 207:108739. https://doi.org/10.1016/j.compscitech.2021.108739
9. Da Costa RMF, Winters A, Hauck B, et al (2021) Biorefining Potential of Wild-Grown Arundo donax, Cortaderia selloana and Phragmites australis and the Feasibility of White-Rot Fungi-Mediated Pretreatments. Front Plant Sci 12:1351. https://doi.org/10.3389/fpls.2021.679966
10. Dünisch O, Baas P (2006) On the origin of intercellular canals in the secondary xylem of selected Meliaceae species. IAWA J 27:281–297. https://doi.org/10.1163/22941932-90000155
11. E. Wheeler (2001) Wood: Macroscopic Anatomy. In: Encyclopedia of Materials: Science and Technology. pp 9653–9657
12. Ferhan, M., Yan, N., & Sain M (2013) A new method for demethylation of lignin from woody biomass using biophysical methods. J Chem Eng Process Technol 4 (5):
13. Frey M, Schneider L, Masania K, et al (2019) Delignified wood-polymer interpenetrating composites exceeding the rule of mixtures. ACS Appl Mater Interfaces 11:35305–35311. https://doi.org/10.1021/acsami.9b11105

14. Frey M, Widner D, Segmehl JS, et al (2018) Delignified and densified cellulose bulk materials with excellent tensile properties for sustainable engineering. ACS Appl Mater Interfaces 10:5030–5037. https://doi.org/10.1021/acsami.7b18646
15. Gibson LJ (2012) The hierarchical structure and mechanics of plant materials. J R Soc Interface 9:2749–2766
16. Grönquist P, Frey M, Keplinger T, Burgert I (2019) Mesoporosity of delignified wood investigated by water vapor sorption. ACS Omega 4:12425–12431. https://doi.org/10.1021/acsomega.9b00862
17. Guan H, Cheng Z, Wang X (2018) Highly compressible wood sponges with a spring-like lamellar structure as effective and reusable oil absorbents. ACS Nano 12:10365–10373. https://doi.org/10.1021/acsnano.8b05763
18. Horikawa Y, Hirano S, Mihashi A, et al (2019) Prediction of Lignin Contents from Infrared Spectroscopy: Chemical Digestion and Lignin/Biomass Ratios of Cryptomeria japonica. Appl Biochem Biotechnol 2019 1884 188:1066–1076. https://doi.org/10.1007/S12010-019-02965-8
19. IAWA Committee (1989) IAWA list of microscopic features for hardwood identification. IAWA Bull n s 10:219–332
20. Icontec (2019a) NTC 784 Maderas. Determinación de la resistencia a la compresión axial o paralela al grano
21. Icontec (2019b) NTC 918 Maderas. Determinación de la dureza (Método Janka)
22. Jakob M, Mahendran AR, Gindl-Altmutter W, et al (2022) The strength and stiffness of oriented wood and cellulose-fibre materials: A review. Prog Mater Sci 125:100916. https://doi.org/10.1016/j.pmatsci.2021.100916
23. Jakob M, Stemmer G, Czabany I, et al (2020) Preparation of high strength plywood from partially delignified densified wood. Polymers (Basel) 12:1796. https://doi.org/10.3390/polym12081796
24. Jamaldheen SB, Kurade MB, Basak B, et al (2022) A review on physico-chemical delignification as a pretreatment of lignocellulosic biomass for enhanced bioconversion. Bioresour Technol 346:126591. https://doi.org/10.1016/j.biortech.2021.126591
25. Jungstedt E, Montanari C, Östlund S, Berglund LA (2020) Mechanical properties of transparent high strength biocomposites from delignified wood veneer. Compos Part A-applied Sci Manuf 133:105853
26. Kim JS, Lee YY, Kim TH (2016) A review on alkaline pretreatment technology for bioconversion of lignocellulosic biomass. Bioresour Technol 199:42–48. https://doi.org/10.1016/j.biortech.2015.08.085
27. Kim S, Kim K, Jun G, Hwang W (2020) Wood-nanotechnology-based membrane for the efficient purification of oil-in-water emulsions. ACS Nano 14:17233–17240. https://doi.org/10.1021/acsnano.0c07206
28. Kumar A, Jyske T, Petrič M (2021) Delignified wood from understanding the hierarchically aligned cellulosic structures to creating novel functional materials: a review. Adv Sustain Syst 5:2000251. https://doi.org/10.1002/adsu.202000251

29. Kumar AK, Sharma S (2017) Recent updates on different methods of pretreatment of lignocellulosic feedstocks: a review. Bioresour Bioprocess 2017 41 4:1–19. https://doi.org/10.1186/S40643-017-0137-9
30. Kutnar A, Sandberg D, Haller P (2015) Compressed and moulded wood from processing to products - a review. Holzforschung 69:885–897. https://doi.org/10.1515/hf-2014-0187
31. Li J, Chen C, Zhu JY, et al (2021) In situ wood delignification toward sustainable applications. Acc Mater Res 2:606–620. https://doi.org/10.1021/accountsmr.1c00075
32. Li J, Wang W, Zhang S, et al (2016) Preparation and characterization of lignin demethylated at atmospheric pressure and its application in fast curing biobased phenolic resins. RSC Adv 6:67435–67443. https://doi.org/10.1039/C6RA11966B
33. Lu Y, Lu YC, Hu HQ, et al (2017) Structural characterization of lignin and its degradation products with spectroscopic methods. J Spectrosc 2017:. https://doi.org/10.1155/2017/8951658
34. Mamoňová M, Reinprecht L (2020) The impact of natural and artificial weathering on the anatomy of selected tropical hardwoods. IAWA J 41:333–355. https://doi.org/https://doi.org/10.1163/22941932-bja10028
35. Mania P, Wróblewski M, Wójciak A, et al (2020) Hardness of densified wood in relation to changed chemical composition. Forests 11:506. https://doi.org/10.3390/F11050506
36. Md Salim R, Asik J, Sarjadi MS (2021) Chemical functional groups of extractives, cellulose and lignin extracted from native Leucaena leucocephala bark. Wood Sci Technol 55:295–313. https://doi.org/10.1007/s00226-020-01258-2
37. Meng Y, Majoinen J, Zhao B, Rojas OJ (2020) Form-stable phase change materials from mesoporous balsa after selective removal of lignin. Compos Part B Eng 199:108296. https://doi.org/10.1016/j.compositesb.2020.108296
38. Okur M, Eslek Koyuncu DD (2020) Investigation of pretreatment parameters in the delignification of paddy husks with deep eutectic solvents. Biomass and Bioenergy 142:105811. https://doi.org/10.1016/j.biombioe.2020.105811
39. Pérez-Escobar OA, Lucas E, Jaramillo C, et al (2019) The Origin and Diversification of the Hyperdiverse Flora in the Chocó Biogeographic Region. Front Plant Sci 10:. https://doi.org/10.3389/FPLS.2019.01328
40. Rabemanolontsoa H, Saka S (2016) Various pretreatments of lignocellulosics. Bioresour Technol 199:83–91. https://doi.org/10.1016/j.biortech.2015.08.029
41. Sandberg D, Haller P, Navi P (2012) Thermo-hydro and thermo-hydro-mechanical wood processing: An opportunity for future environmentally friendly wood products. Wood Mater Sci Eng 8:64–88. https://doi.org/10.1080/17480272.2012.751935
42. Schneider CA, Rasband WS, Eliceiri KW (2012) NIH Image to ImageJ: 25 years of image analysis. Nat Methods 2012 97 9:671–675. https://doi.org/10.1038/NMETH.2089
43. Senthilkumar ER (2019) The Effect of Calcium on Delignification in Kraft Cooking of Eucalyptus. KTH, School of Engineering Sciences in Chemistry, Biotechnology and Health (CBH)

44. Shams MI, Yano H, Endou K (2005) Compressive deformation of wood impregnated with low molecular weight phenol formaldehyde (PF) resin III: effects of sodium chlorite treatment. J Wood Sci 51:234–238. https://doi.org/10.1007/s10086-004-0638-y
45. Shi J, Lu Y, Zhang Y, et al (2018) Effect of thermal treatment with water, H2SO4 and NaOH aqueous solution on color, cell wall and chemical structure of poplar wood. Sci Reports 2018 81 8:1–9. https://doi.org/10.1038/s41598-018-36086-9
46. Shi J, Peng J, Huang Q, et al (2020) Fabrication of densified wood via synergy of chemical pretreatment, hot-pressing and post mechanical fixation. J Wood Sci 66:5. https://doi.org/10.1186/s10086-020-1853-x
47. Siedlecka A, Wiklund S, Péronne M-A, et al (2008) Pectin Methyl Esterase Inhibits Intrusive and Symplastic Cell Growth in Developing Wood Cells of Populus. Plant Physiol 146:323–324. https://doi.org/10.1104/pp.107.111963
48. Singh R, Shukla A, Tiwari S, Srivastava M (2014) A review on delignification of lignocellulosic biomass for enhancement of ethanol production potential. Renew Sustain Energy Rev 32:713–728. https://doi.org/10.1016/j.rser.2014.01.051
49. Song J, Chen C, Wang C, et al (2017) Superflexible Wood. ACS Appl Mater Interfaces 9:23520–23527. https://doi.org/10.1021/acsami.7b06529
50. Song J, Chen C, Yang Z, et al (2018a) Highly Compressible, Anisotropic Aerogel with Aligned Cellulose Nanofibers. ACS Nano 12:140–147. https://doi.org/10.1021/acsnano.7b04246
51. Song J, Chen C, Zhu S, et al (2018b) Processing bulk natural wood into a high-performance structural material. Nature 554:224–228. https://doi.org/10.1038/nature25476
52. Sun N, Rahman M, Qin Y, et al (2009) Complete dissolution and partial delignification of wood in the ionic liquid 1-ethyl-3-methylimidazolium acetate. Green Chem 11:646–655. https://doi.org/10.1039/B822702K
53. Thomas DS, Montagu KD, Conroy JP (2007) Temperature effects on wood anatomy, wood density, photosynthesis and biomass partitioning of Eucalyptus grandis seedlings. Tree Physiol 27:251–260. https://doi.org/10.1093/treephys/27.2.251
54. Van Soest PJ, Robertson JB, Lewis BA (1991) Methods for dietary fiber, neutral detergent fiber, and nonstarch polysaccharides in relation to animal nutrition. J Dairy Sci 74:3583–3597. https://doi.org/10.3168/jds.S0022-0302(91)78551-2
55. Wagih A, Hasani M, Hall SA, Theliander H (2021) Micro/nano-structural evolution in spruce wood during soda pulping. Holzforschung 75:754–764. https://doi.org/doi:10.1515/hf-2020-0113
56. Wang J, Fishwild SJ, Begel M, Zhu JY (2020) Properties of densified poplar wood through partial delignification with alkali and acid pretreatment. J Mater Sci 55:14664–14676. https://doi.org/10.1007/s10853-020-05034-2
57. Wang J, Liu J, Li J, Zhu JY (2021a) Characterization of microstructure, chemical, and physical properties of delignified and densified poplar wood. Materials (Basel) 14:. https://doi.org/10.3390/ma14195709

58. Wang K, Dong Y, Ling Z, et al (2021b) Transparent wood developed by introducing epoxy vitrimers into a delignified wood template. Compos Sci Technol 207:. https://doi.org/10.1016/j.compscitech.2021.108690
59. Wheeler EA (2011) Inside Wood – A Web resource for hardwood anatomy. IAWA J 32:199–211. https://doi.org/https://doi.org/10.1163/22941932-90000051
60. Wu J, Wu Y, Yang F, et al (2019) Impact of delignification on morphological, optical and mechanical properties of transparent wood. Compos Part A Appl Sci Manuf 117:324–331. https://doi.org/10.1016/j.compositesa.2018.12.004
61. Xu F (2010) Structure, Ultrastructure, and Chemical Composition. In: Cereal Straw as a Resource for Sustainable Biomaterials and Biofuels. Elsevier, pp 9–47
62. Yang R, Cao Q, Liang Y, et al (2020) High capacity oil absorbent wood prepared through eco-friendly deep eutectic solvent delignification. Chem Eng J 401:126150. https://doi.org/10.1016/j.cej.2020.126150
63. Zanne AE, Westoby M, Falster DS, et al (2010) Angiosperm wood structure: Global patterns in vessel anatomy and their relation to wood density and potential conductivity. Am J Bot 97:207–215. https://doi.org/10.3732/ajb.0900178
64. Zhao L, Sun ZF, Zhang CC, et al (2022) Advances in pretreatment of lignocellulosic biomass for bioenergy production: Challenges and perspectives. Bioresour Technol 343:. https://doi.org/10.1016/j.biortech.2021.126123
65. Zhu J, Guo F, Ma C, et al (2022) The alkaline extraction efficiency of bamboo cell walls is related to their structural differences on both anatomical and molecular level. Ind Crops Prod 178:114628. https://doi.org/10.1016/j.indcrop.2022.114628
66. Zhuang J, Li M, Pu Y, et al (2020) Observation of Potential Contaminants in Processed Biomass Using Fourier Transform Infrared Spectroscopy. Appl Sci 10:. https://doi.org/10.3390/app10124345

Figures

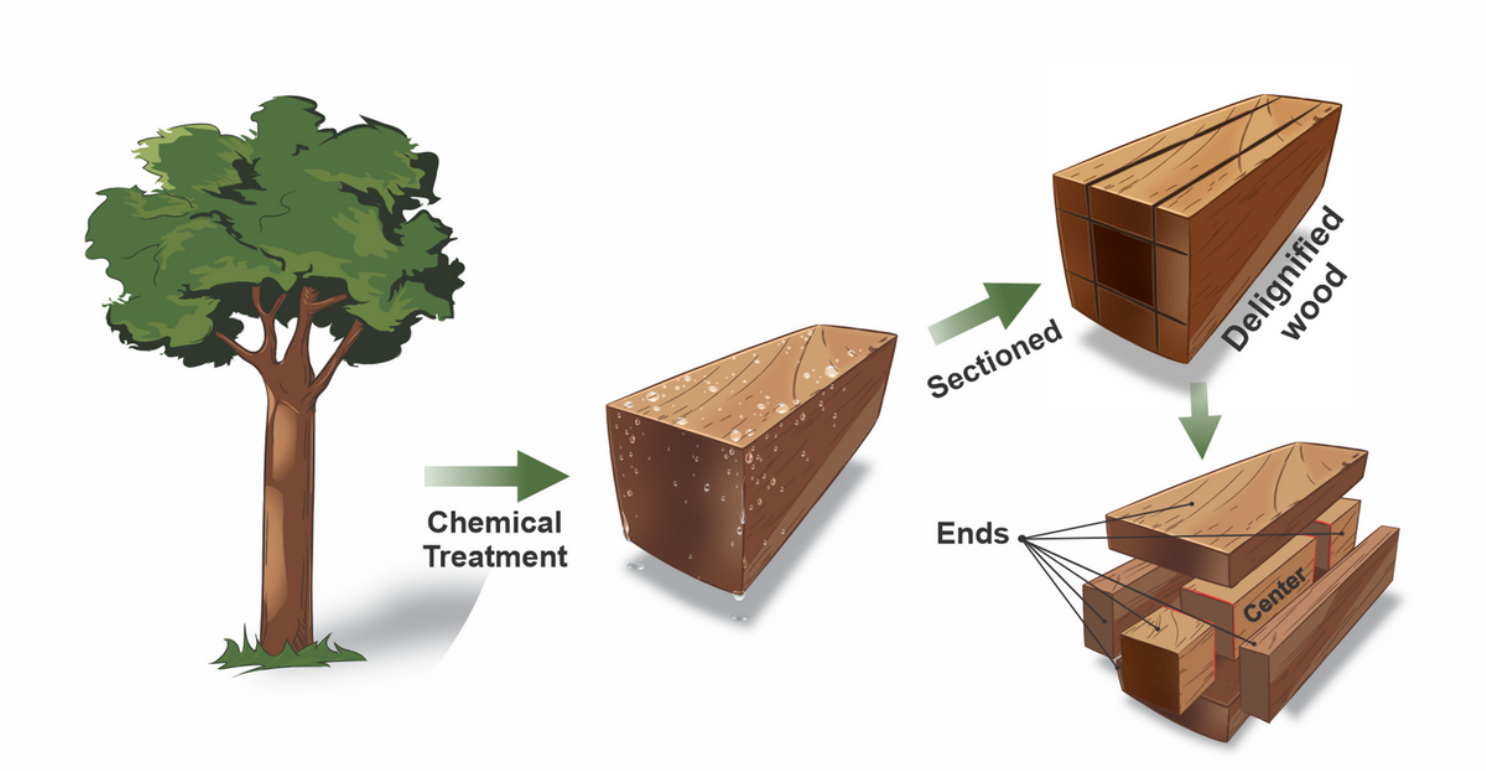

Figure 1

Schematic illustration of delignified wood sectioning. The process involves studying delignified wood by comparing the differences observed between the ends and the center of the wood samples.

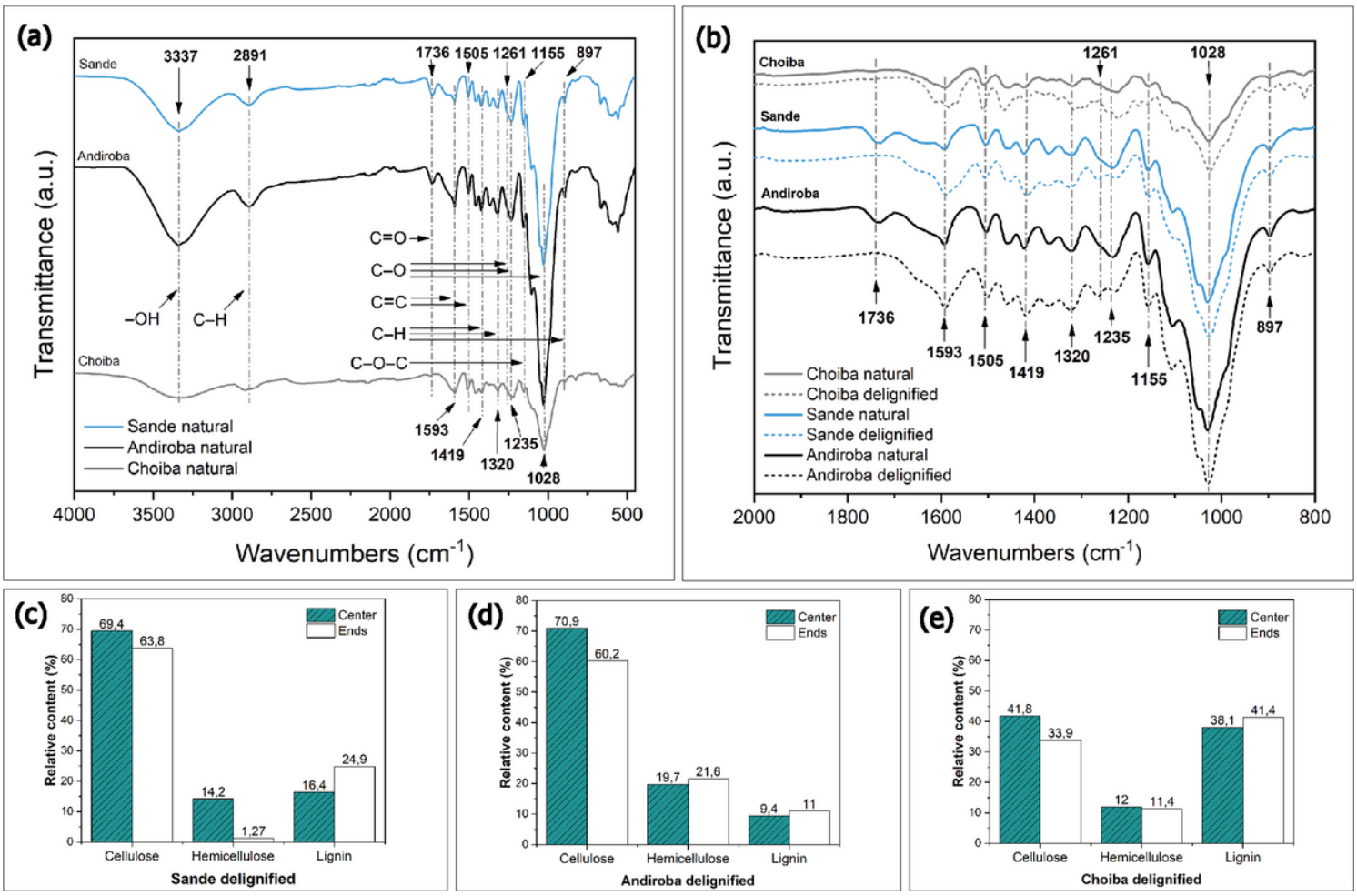

Figure 2

FT-IR spectra of (a) natural wood and (b) delignified wood. (c-e) Comparison of the relative content of cellulose, hemicelluloses, and lignin in different wood samples obtained from the chemical composition of the ends and centers of delignified wood.

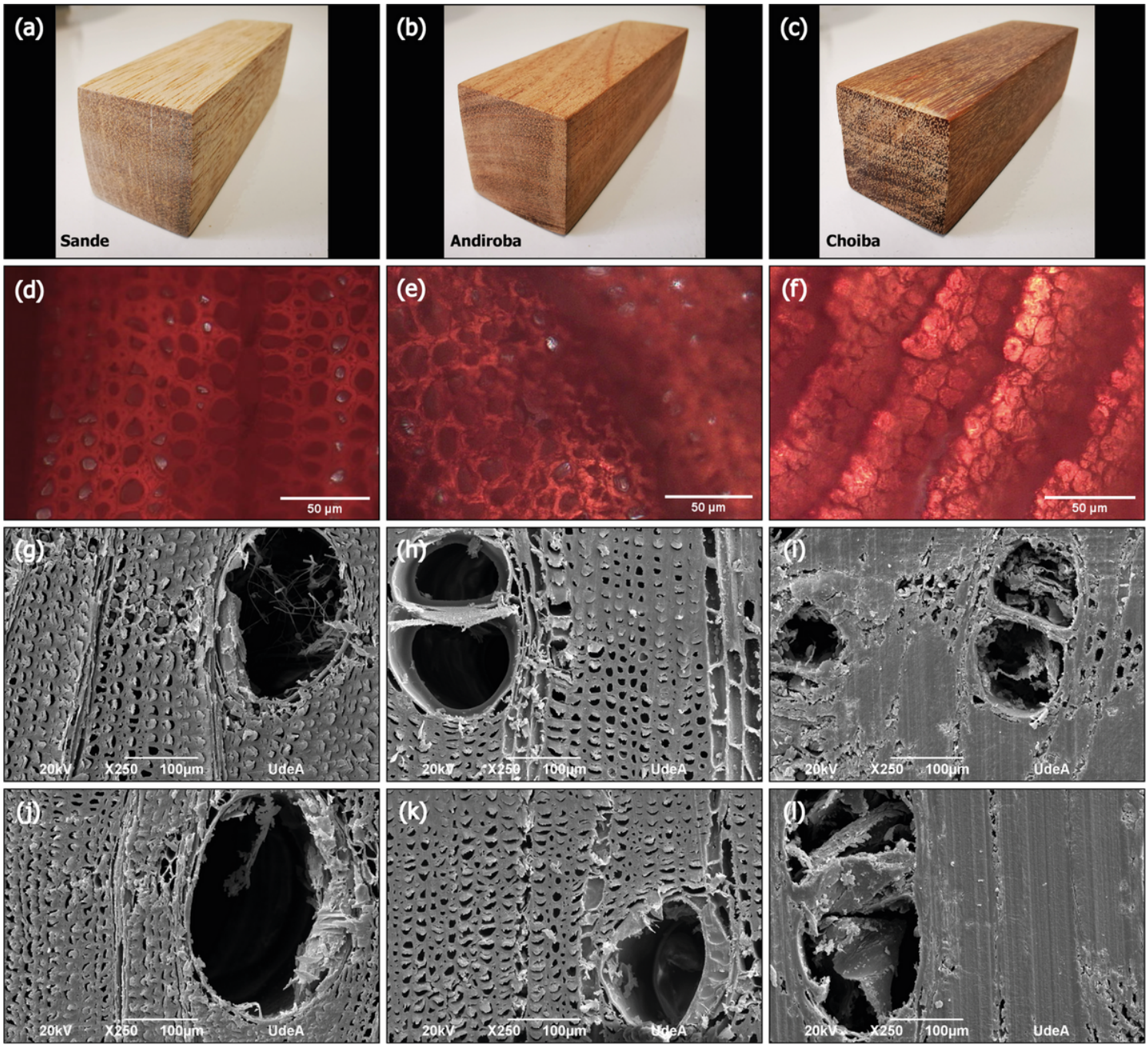

Figure 3

Morphology and structure of different wood samples: (a-c) photographs of natural wood showing cross-section, radial, and longitudinal section of samples; (d-e) cross-sectional optical images showing lumen structure and wood fibers; (g-i) SEM images showing the honeycomb-like structure of natural wood; (j-l) SEM images showing the preserved structure of the woods after delignification treatment.

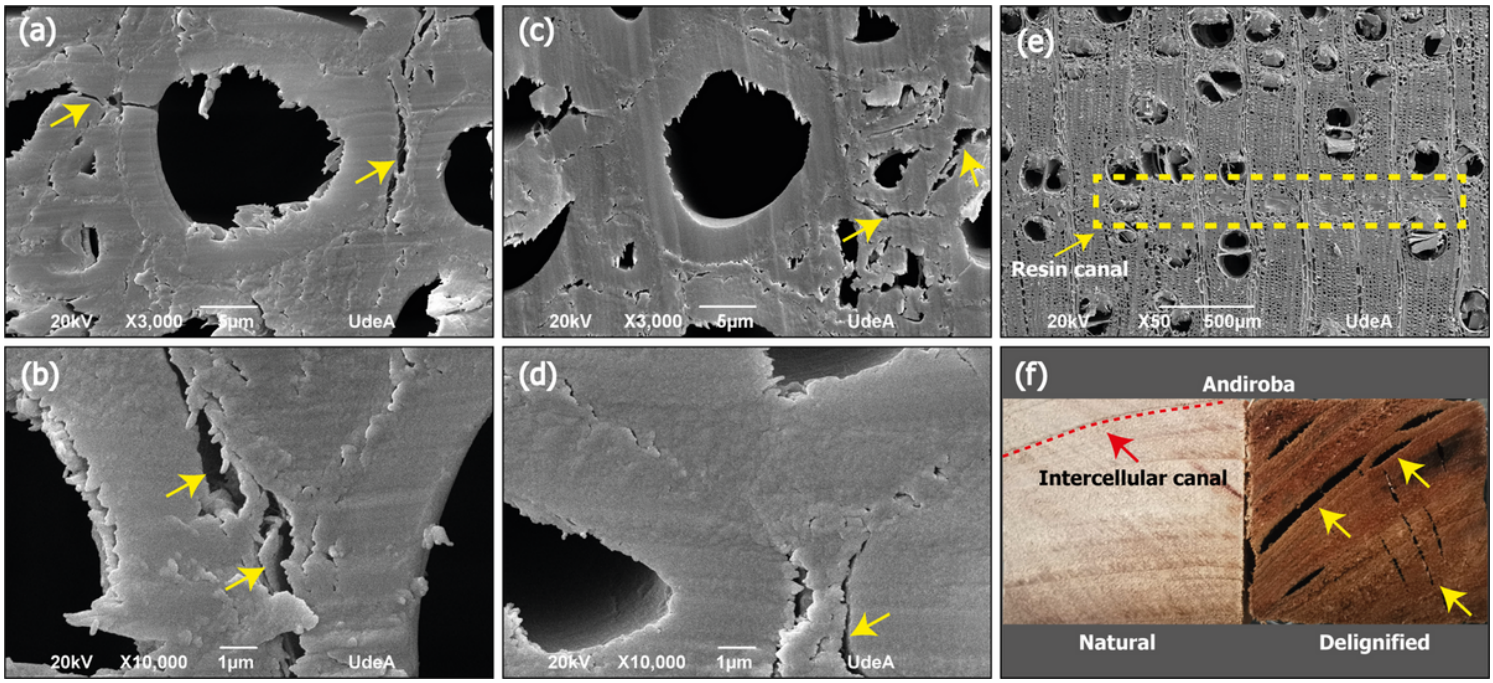

Figure 4

Effects of partial delignification on wood structure: a) and b) SEM images showing the preserved structure of delignified Sande; c) and d) SEM images showing the preserved structure of delignified Andiroba; e) photograph showing a band of traumatic intercellular canals (tangential line of axial resin canals) in Andiroba wood; f) photograph showing delamination effects in traumatic channels of delignified andiroba cross-section.

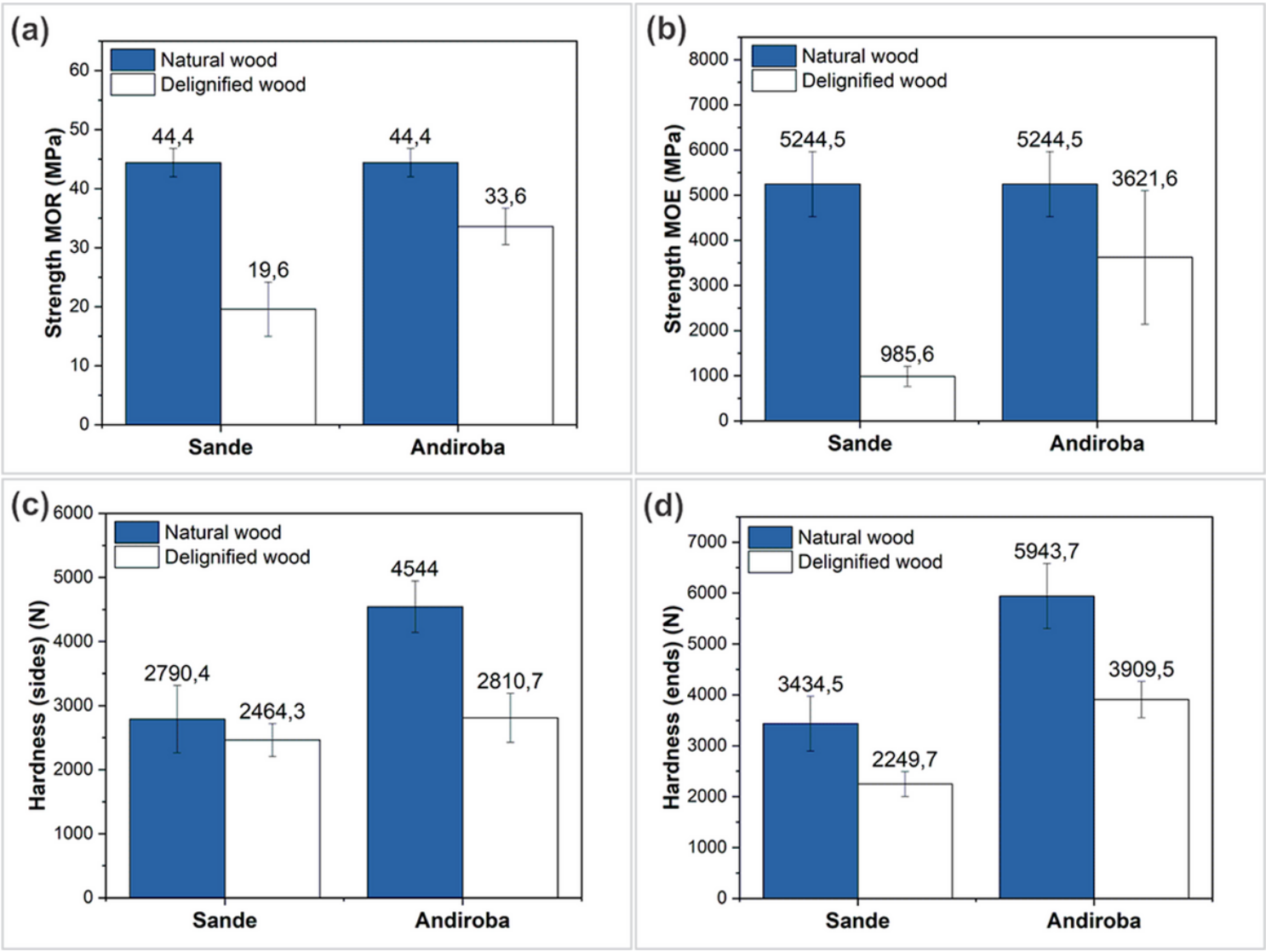

Figure 5

Effects of partial delignification on the mechanical properties of natural wood: (a) and (b) Comparison of MOR and MOE derived from compressive tests; (c) and (d) Comparison of Janka hardness measured in the sides and ends of woods samples.